Implementation of the KASKAD Computer Code System for WWER-440 at Kozloduy NPP

A. Antov, N. Georgieva, V. Spasova

Kozloduy NPP, Kozloduy, Bulgaria

1. Introduction

Since 2002 at Kozloduy NPP – EP1 the code package KASKAD is used for WWER-440 reactor core calculations. The main codes entering this package are:

- BIPR-7A: 3-D diffusion and core analysis code;
- PERMAK-A: 2-D fine mesh diffusion code.

The burnup calculations were performed for all cycles of the Kozloduy NPP Unit 1, Unit 2, Unit 3 and Unit 4. For the last 4-5 cycles of the Units were calculated control rods worth, critical boron concentration at zero power, reactivity coefficients and linear power. These results were analysed and were compared with experimental data. Some results were given in this paper.

2. Results

2.1. Burnup Distribution

Figures 1-6 show loading pattern and burn-up distribution [MWd/kgU, BOC] of assemblies for cycles 16-18 of Unit 3 and cycle 15-17 of Unit 4.

2.2. Boric Acid Concentration

Table 1 shows the comparison between the measured and predicted critical boric acid concentration at BOC zero power states. The difference between measurement and calculated boric acid concentration is about 0.3 g/kg.

The measured and calculated boric acid concentration during Cycles 16-18 of Unit 3 and Cycles 15-17 of Unit 4 can be seen in Figures 7-12. The measured boric acid concentration is smaller than the calculated one at BOC starting from 0 FPD to 60-80 FPD, after that it is bigger. The average difference between measured and calculated boric acid concentration is 0.3 g/kg.

2.3. Relative Power Distribution

In Figures 14-19 are presented deviations between measurements and calculations for the power peaking factors by assembly types $\Delta=(K_q^{meas}-K_q^{exp})\cdot 100\%$ for selected FPD for Cycles 16-18 of Unit 3 and Cycles 14, 15 and 17 of Unit 4.

2.4. Control Rods Worth

The measured and calculated integral and differential efficiencies of group 6 at Hot Zero Power BOC are presented in Figures 7-12. The measured integral efficiencies are bigger than the calculated ones approximately 10%.

2.5. Linear Power Distribution

The linear power and permissible maximum linear power dependences on the average fuel rod burnup are demonstrated in Figures 20-25. The calculated linear power is smaller than the permissible maximum linear power for all the cycles of Units 1-4.

3. Conclusions

A series of calculations and analyses using the code package system KASKAD for all the cycles of Units 1-4 show that the agreement between measured and calculated results is good. The code package system KASKAD is used in Kozloduy NPP, EP-1, for neutron-physics calculations, independently of the computer code system SPPS1.6 & HEXAB2DB for the safety evaluation of the core loading patterns of reactors WWER-440.

4. References

[1] Н. Бычкова, М. Томилов. Комплекс программ нейтронно-физических расчетов РНЦКИ. Комплекс программ КАСКАД. Инструкция по изполозованию графического интерфейса комплекса КАСКАД. Москва, 2002.

[2] А. Суслов, Л. Шишков, С. Большагин. Комплекс программ нейтронно-физических расчетов РНЦКИ. Комплекс программ КАСКАД. Программа БИПР-7А. Москва, 2002.

[3] С. Алешин, С. Большагин, М. Томилов. Комплекс программ нейтронно-физических расчетов РНЦ КИ. Программа ПЕРМАК-А. Описание алгоритма и инструкция для пользователя.

[4] А. Марков, М. Томилов. Комплекс программ нейтронно-физических расчетов РНЦКИ. Программа ПИР-А. Описание алгоритма и применения. Москва, 2001.

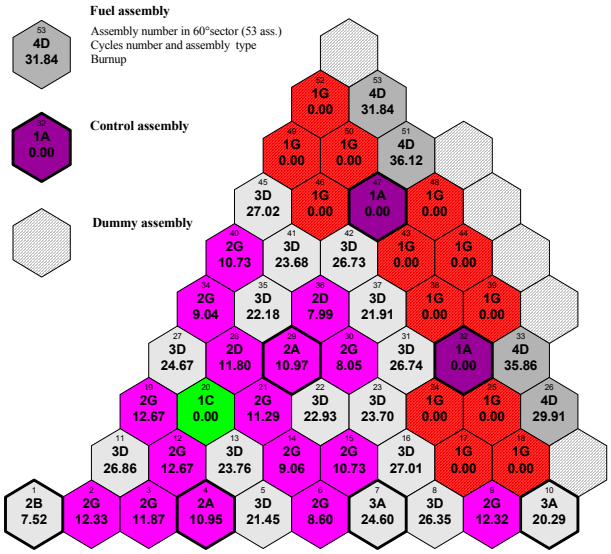

A - 3.6% wall thickness 2.1mm with St. steel spacer grids
B- 2.4% wall thickness 2.1mm with St. steel spacer grids
D - 3.6% wall thickness 1.5mm with St. steel spacer grids
E - 2.4% wall thickness 1.5mm with St. steel spacer grids
F - 1.6% wall thickness 1.5mm with St. steel spacer grids
G - 3.6% wall thickness 1.5mm and Zr spacer grids
H - 2.4% wall thickness 1.5mm and Zr spacer grids
J - 3.6% wall thickness 2.0mm and Zr spacer grids

Figure 1. Core loading pattern and assembly burnup [MWd/kgU, BOC] for the 16-th fuel cycle of Unit 3

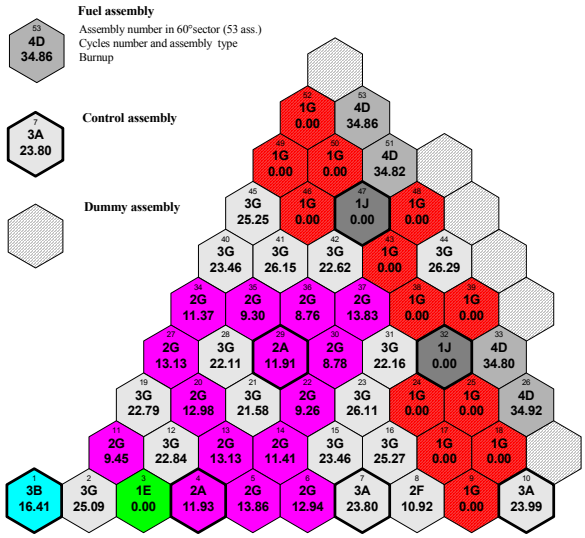

A - 3.6% wall thickness 2.1mm with St. steel spacer grids
B- 2.4% wall thickness 2.1mm with St. steel spacer grids
C- 1.6% wall thickness 2.1mm with St. steel spacer grids
D - 3.6% wall thickness 1.5mm with St. steel spacer grids
E - 2.4% wall thickness 1.5mm with St. steel spacer grids
F - 1.6% wall thickness 1.5mm with St. steel spacer grids
G - 3.6% wall thickness 1.5mm and Zr spacer grids
H - 2.4% wall thickness 1.5mm and Zr spacer grids
J - 3.6% wall thickness 2.0mm and Zr spacer grids

Figure 2. Core loading pattern and assembly burnup [MWd/kgU, BOC] for the 17-th fuel cycle of Unit 3

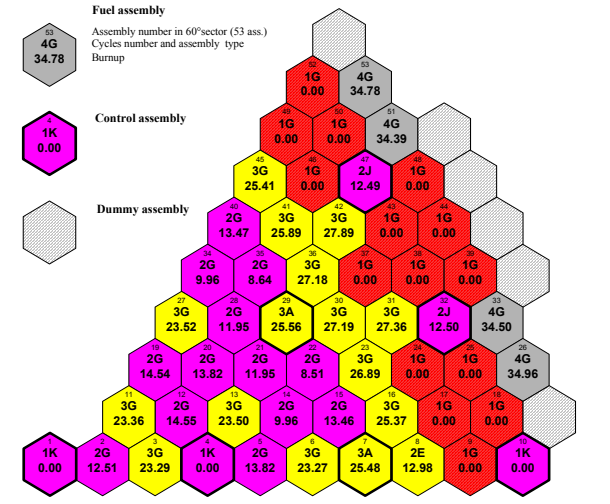

A - 3.6% wall thickness 2.1mm with St. steel spacer grids
E - 2.4% wall thickness 1.5mm with St. steel spacer grids
G - 3.6% wall thickness 1.5mm and Zr spacer grids
H - 2.4% wall thickness 1.5mm and Zr spacer grids
J - 3.6% wall thickness 2.0mm and Zr spacer grids
K - 2.4% wall thickness 2.0mm and Zr spacer grids

Figure 3. Core loading pattern and assembly burnup [MWd/kgU, BOC] for the 18-th fuel cycle of Unit 3

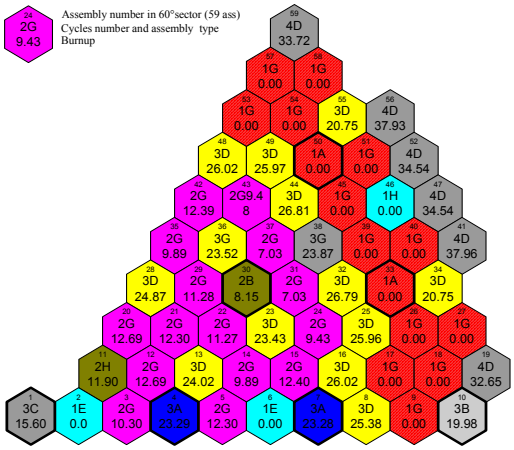

A - 3.6% wall thickness 2.1mm with St.steel spacer grids
B- 2.4% wall thickness 2.1mm with St.steel spacer grids
C- 1.6% wall thickness 2.1mm with St.steel spacer grids
D - 3.6% wall thickness 1.5mm with St.steel spacer grids
E - 2.4% wall thickness 1.5mm with Steel spacer grids
G - 3.6% wall thickness 1.5mm and Zr spacer grids
H - 2.4% wall thickness 1.5mm and Zr spacer grids

Figure 4. Core loading pattern and assembly burnup [MWd/kgU, BOC] for the 15-th fuel cycle of Unit 4

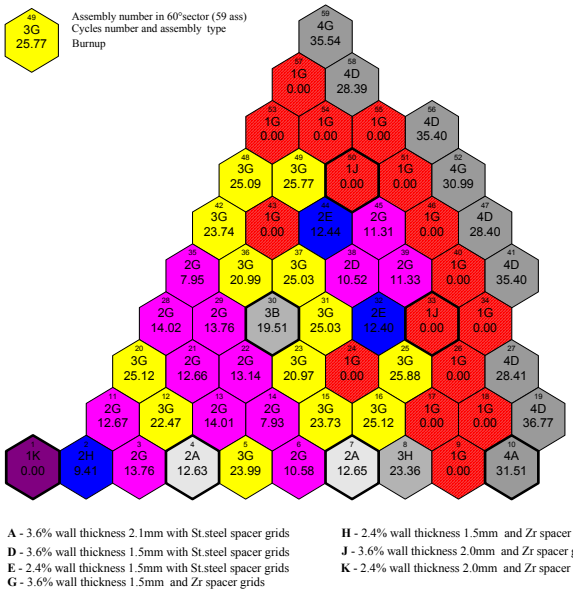

Figure 5. Core loading pattern and assembly burnup [MWd/kgU, BOC] for the 16-th fuel cycle of Unit 4

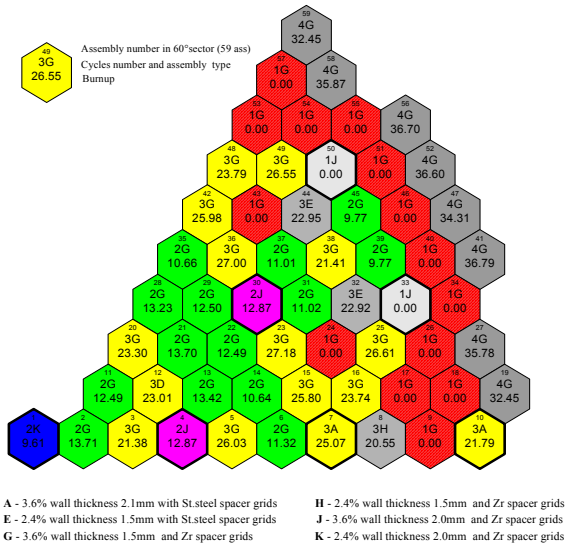

Figure 6. Core loading pattern and assembly burnup [MWd/kgU, BOC] for the 17-th fuel cycle of Unit 4

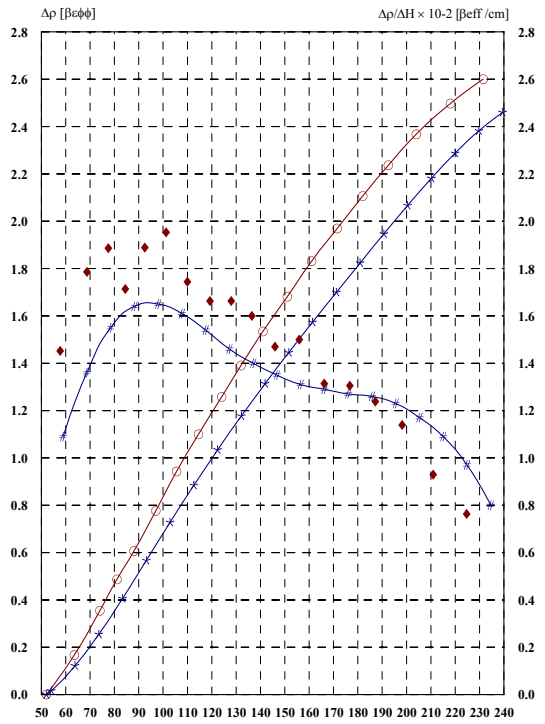

Figure 7. Measured and calculated differential and integral efficiency 6-th group control rod Cycle 16 of Unit 3 (BOC, N_t = 0%)

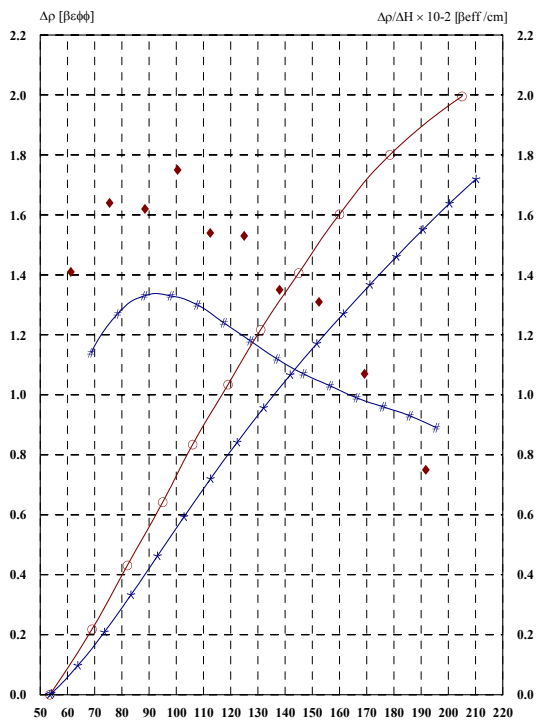

Figure 8. Measured and calculated differential and integral efficiency 6-th group control rod Cycle 17 of Unit 3 (BOC, N_t = 0%)

* – $\Delta\rho$ [beff] - BIPR7A
o – $\Delta\rho$ [beff] - meas.
\# – $\Delta\rho/\Delta H \cdot 10^{-2}$[beff/cm] - BIPR7A
♦ – $\Delta\rho/\Delta H \cdot 10^{-2}$ [beff/cm] - meas.

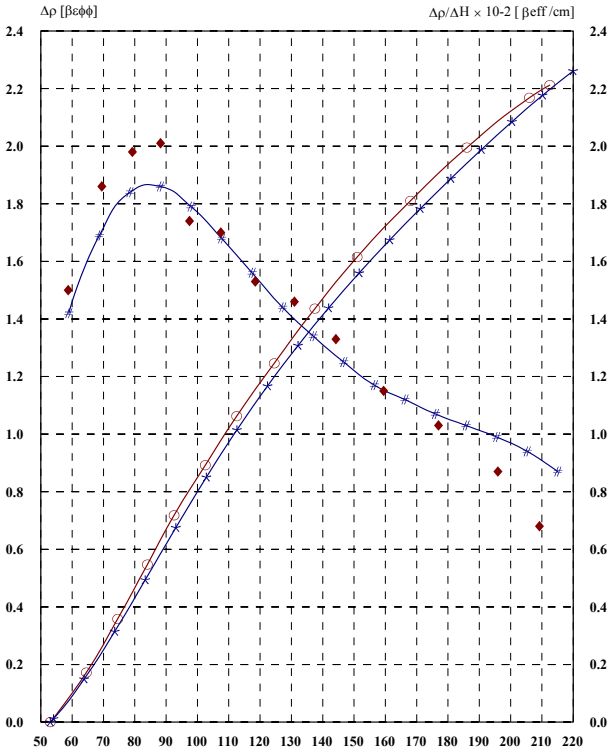

Figure 9. Measured and calculated differential and integral efficiency 6-th group control rod Cycle 17 of Unit 3 (BOC, N_t = 0%)

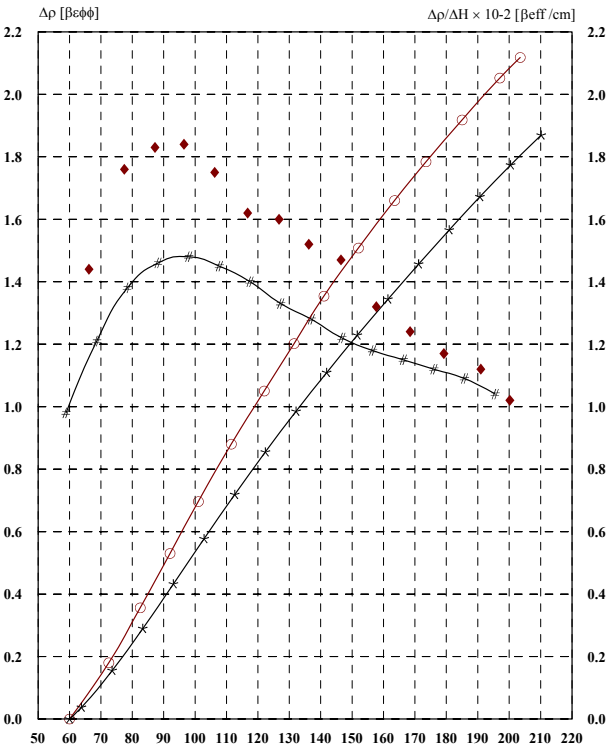

Figure 10. Measured and calculated differential and integral efficiency 6-th group control rod Cycle 15 of Unit 3 (BOC, N_t = 0%)

*** – $\Delta\rho$ [beff] - BIPR7A # – $\Delta\rho/\Delta H \cdot 10^{-2}$ [beff/cm] - BIPR7A**
o – $\Delta\rho$ [beff] - meas. ♦ – $\Delta\rho/\Delta H \cdot 10^{-2}$ [beff/cm] - meas.

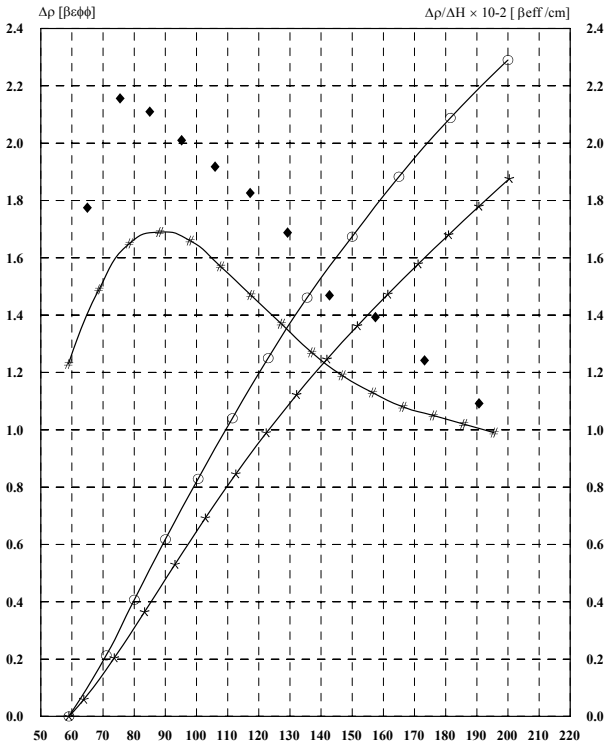

Figure 11. Measured and calculated differential and integral efficiency 6-th group control rod Cycle 16 of Unit 4 (BOC, N_t = 0%)

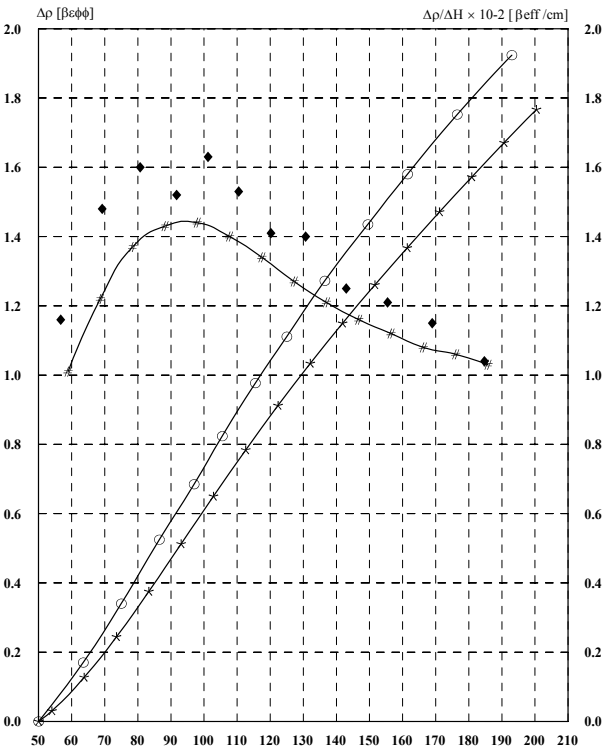

Figure 12. Measured and calculated differential and integral efficiency 6-th group control rod Cycle 17 of Unit 4 (BOC, N_t = 0%)

*** – $\Delta\rho$ [beff] - BIPR7A # – $\Delta\rho/\Delta H \cdot 10^{-2}$ [beff/cm] - BIPR7A**
o – $\Delta\rho$ [beff] - meas. ♦ – $\Delta\rho/\Delta H \cdot 10^{-2}$ [beff/cm] - meas.

Table 1. Measurement and calculation of critical boric acid for cycles 16, 17, 18 of Unit 3 and cycles 15, 16, 17 of Unit 4 (BOC, N_t = 0%)

Unit №	Cycle №	$T_{inp.}$ [°C]	H_{VI} [cm]	$H_{12\text{-}43}$ [cm]	$C^{exp}_{H_3BO_3}$ [g/kg]	$C^{calc}_{H_3BO_3}$ [g/kg]	$\Delta = C^{exp}_{H_3BO_3} - C^{calc}_{H_3BO_3}$ [g/kg]
3	16	260.3	191.0	191.0	8.77	8.66	0.11
		259.0	125.0	125.0	8.37	8.26	0.11
		260.6	220.0	100.0	8.77	8.71	0.06
		250.5	222.0	115.0	8.77	8.75	0.02
		259.3	222.0	175.5	8.77	8.78	-0.01
		258.8	183.5	183.5	8.43	8.63	-0.20
		258.6	49.0	49.0	7.81	7.77	0.04
		259.4	226.5	226.5	8.77	8.89	-0.12
	17	259.0	195.0	195.0	9.17	8.97	0.20
		260.0	193.5	100.0	9.17	8.90	0.27
		251.0	183.0	85.5	8.68	8.88	-0.20
		258.7	183.0	167.5	8.68	8.92	-0.24
		252.4	53.5	53.5	8.18	8.27	-0.09
		252.5	205.0	205.0	8.92	9.02	-0.10
	18	262.0	183.0	183.0	8.62	8.62	0.00
		257.2	182.5	100.0	8.68	8.52	0.16
		250.8	193.0	115.0	8.62	8.59	0.03
		259.7	193.0	173.0	8.62	8.63	-0.01
		259.3	53.0	53.0	7.75	7.76	-0.01
		259.0	212.0	212.0	8.68	8.75	-0.07
		260.8	223.0	223.0	8.68	8.79	-0.11
4	15	260.0	175.0	175.0	8.42	8.90	-0.48
		260.5	190.0	100.0	8.42	8.94	-0.52
		251.0	195.5	75.0	8.55	8.94	-0.39
		260.4	195.5	137.5	8.55	8.97	-0.42
		260.7	183.0	183.0	8.92	8.96	-0.04
		258.3	60.0	60.0	8.27	8.25	0.02
		258.1	203.5	203.5	9.08	9.06	0.02
	16	257.0	190.0	190.0	8.68	8.68	0.00
		257.0	190.0	190.0	8.54	8.68	-0.14
		257.0	122.0	122.0	8.25	8.32	-0.07
		261.5	223.0	100.0	8.42	8.69	-0.27
		251.2	198.0	104.0	8.47	8.65	-0.18
		259.0	198.0	145.5	8.47	8.66	-0.19
		256.4	59.0	59.0	7.77	7.97	-0.20
		257.0	205.5	205.5	8.67	8.77	-0.10
	17	256.6	190.0	190.0	8.43	8.59	-0.16
		253.0	187.0	100.0	8.43	8.50	-0.07
		251.9	189.0	106.5	8.43	8.50	-0.07
		260.4	189.0	163.0	8.43	8.57	-0.14
		260.0	50.0	50.0	7.69	7.81	-0.12
		258.5	193.0	193.0	8.37	8.58	-0.21
		258.4	187.5	187.5	8.30	8.58	-0.28

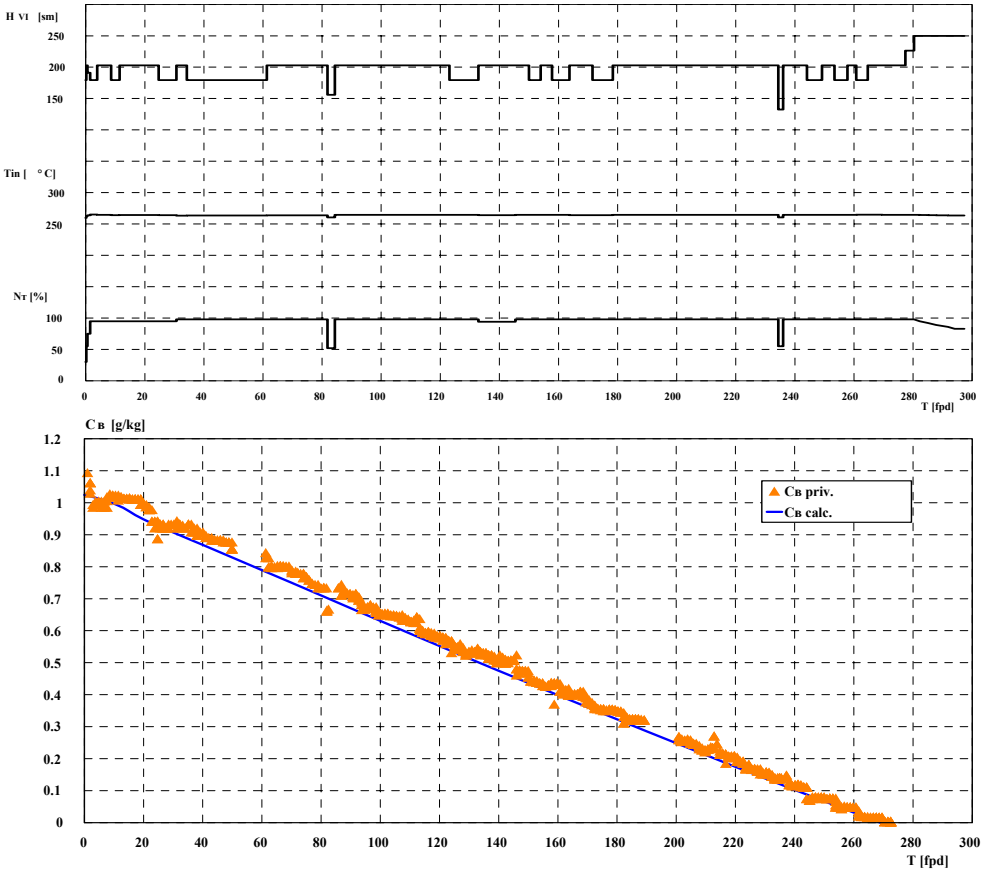

Figure 13. Determined measured critical boron concentration *Cb* priv. to compare to the predicted critical boron concentration $C_{b,calc.}$ for Cycle 22 of Unit 1

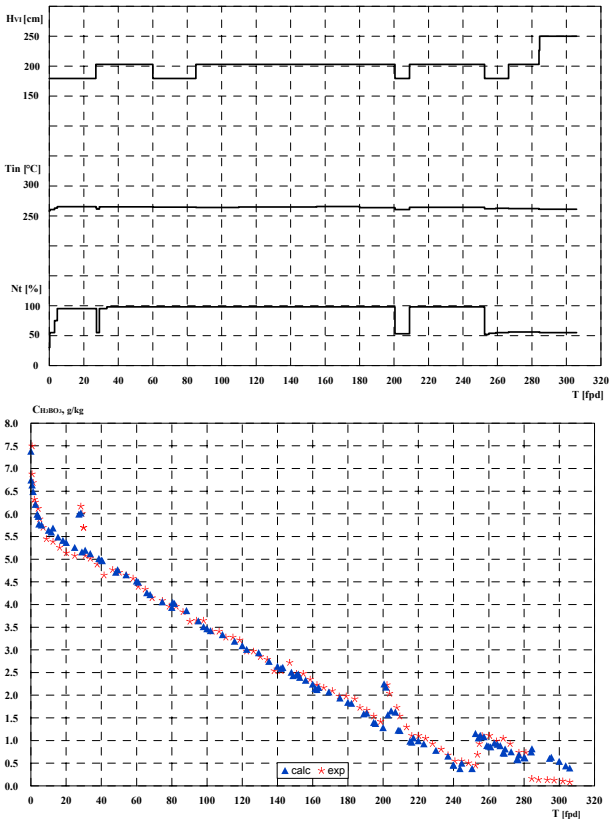

Figure 14. Operation regime and comparison of calculated and measured boric acid concentration for Cycle 16 of Unit 3

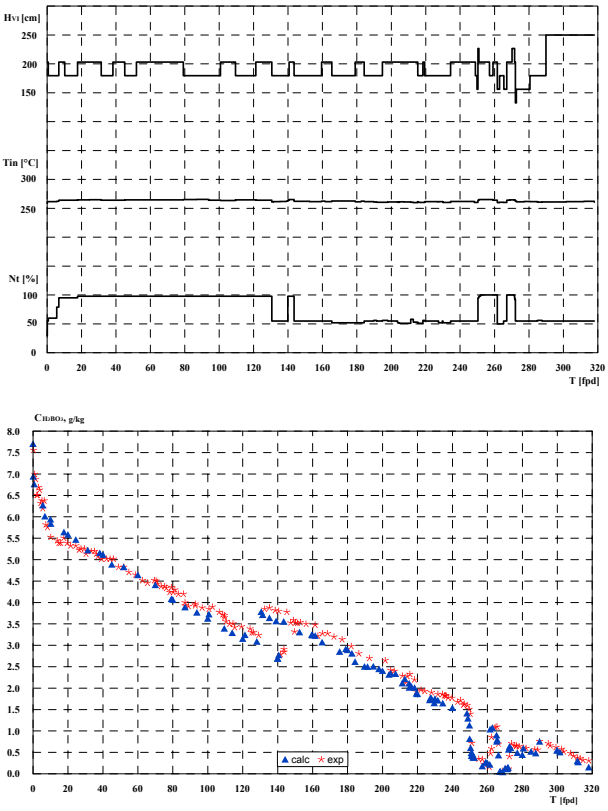

Figure 15. Operation regime and comparison of calculated and measured boric acid concentration for Cycle 17 of Unit 3

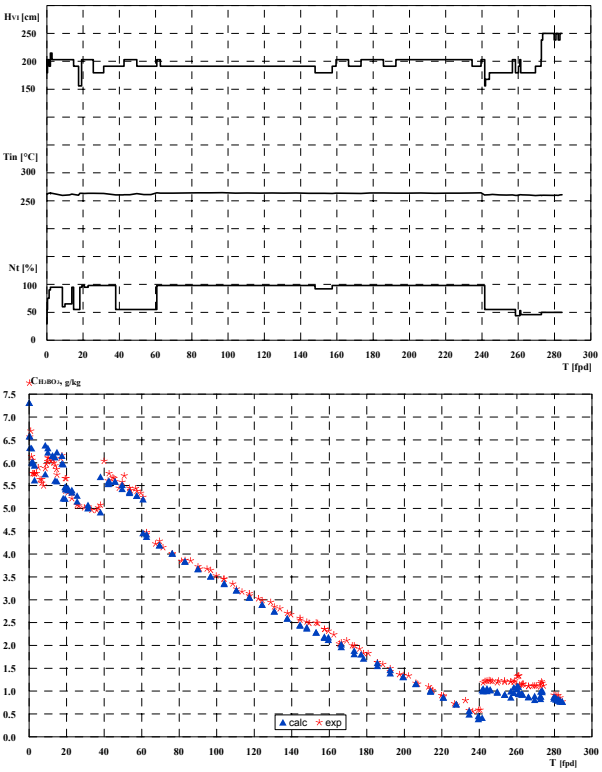

Figure 16. Operation regime and comparison of calculated and measured boric acid concentration for Cycle 18 of Unit 3

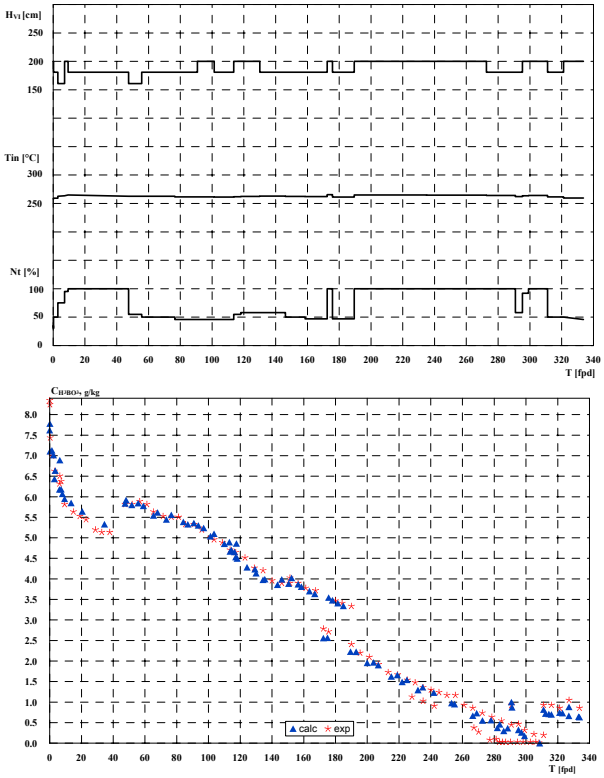

Figure 17. Operation regime and comparison of calculated and measured boric acid concentration for Cycle 15 of Unit 4

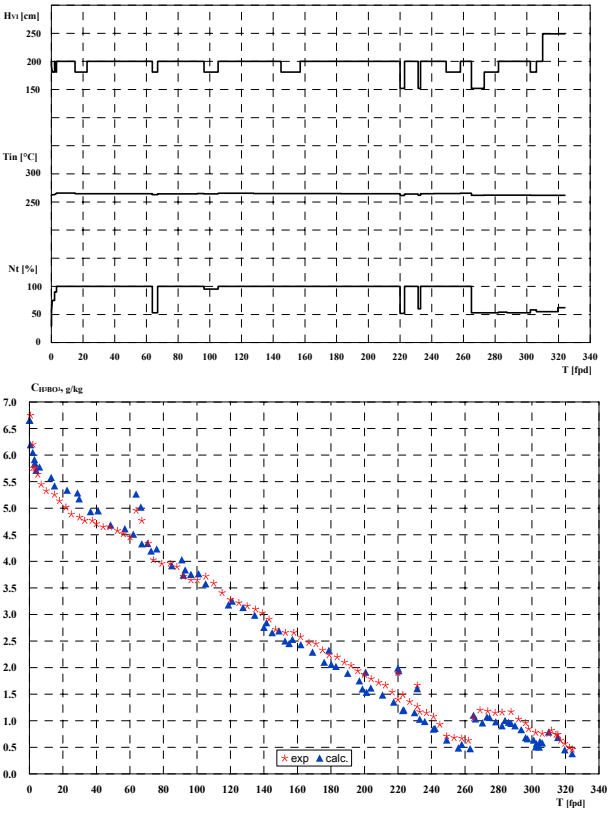

Figure 18. Operation regime and comparison of calculated and measured boric acid concentration for Cycle 16 of Unit 4

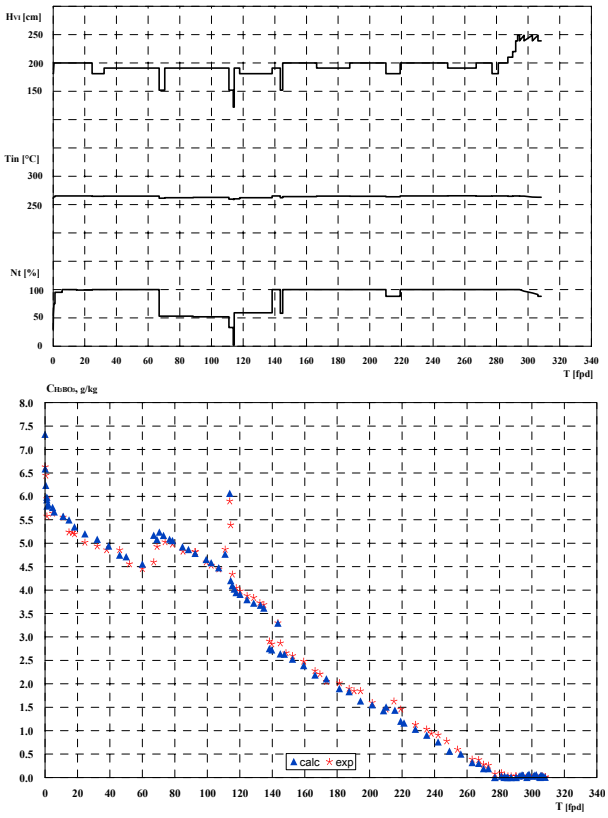

Figure 19. Operation regime and comparison of calculated and measured boric acid concentration for Cycle 17 of Unit 4

Table 2. Average deviation between measurement and calculation power peaking factors by assembly types for Cycle 16 of Unit 3 ($\Delta=K_q^{meas}-K_q^{exp}$)·100

T_{ef}, [FPD]	Cycle, Assembly type	6.0	25.8	37.9	78.5	119.6	160.5	201.1	220.2	255.1	264.3
T_{in}, [°C]		264.4	264.9	265.1	265	264.3	265.5	260.6	264.5	262	262.8
H_{VI}, [cm]		181	181	181	181	200	200	162	200	191	200
N_t, [%]		95	95	98	98	98	98	53	98	54	55
Average Deviation, [%]	1G	-0.7	-0.3	-0.4	-1.6	-2.8	-4.0	-7.0	-5.2	-8.0	-7.8
	2G	-4.6	-5.0	-4.6	-4.2	-3.5	-2.9	-1.2	-2.2	-0.7	0.2
	3D	2.2	2.3	1.8	2.4	2.6	2.9	3.4	2.2	3.1	2.7
	4D	8.4	7.3	8.2	9.3	10.5	12.7	14.5	16.3	15.1	16.9

Table 3. Average deviation between measurement and calculation power peaking factors by assembly types for Cycle 17 of Unit 3 ($\Delta=K_q^{meas}-K_q^{exp}$)·100

T_{ef}, [FPD]	Cycle, Assembly type	8.3	43.0	111.5	184.3	238.1	252.1	268.2	276.5	293.2	315.3
T_{in}, [°C]		264.1	264.6	264.9	261.7	262.2	265.2	264.5	261.9	261.4	262.0
H_{VI}, [cm]		191	200	190	181	200	191	210	152	250	250
N_t, [%]		95	98	98	55	55	100	100	55	55	55
Average Deviation, [%]	1G	1.8	2.1	-0.4	-3.3	-2.8	-4.2	-4.2	-4.8	-6.6	-6.0
	2G	-3.5	-3.3	-1.9	-0.1	-0.1	-0.4	-0.1	1.3	1.3	1.9
	3G	-0.2	0.2	1.2	1.9	2.0	3.4	3.4	2.8	3.5	3.4
	4D	5.9	4.2	3.5	2.5	2.2	2.7	2.6	1.3	2.6	0.7

Table 4. Average deviation between measurement and calculation power peaking factors by assembly types for Cycle 18 of Unit 3 ($\Delta=K_q^{meas}-K_q^{exp}$)·100

T_{ef}, [FPD]	Cycle, Assembly type	0.1	3.9	18.0	39.9	62.5	94.8	122.2	173.2	205.2	225.7
T_{in}, [°C]		262.8	263.4	263.4	260.0	263.9	264.5	264.1	263.3	264.2	264.2
H_{VI}, [cm]		181	191	152	191	200	191	191	200	191	200
N_t, [%]		55	95	95	55	98	98	98	98	98	98
Average Deviation, [%]	1G	-2.6	-2.7	-4.5	-3.7	-4.1	-4.9	-5.7	-5.8	-6.6	-6.6
	2G	2.3	1.3	2.3	2.6	1.6	2.2	2.8	3.3	2.8	3.2
	3G	-0.5	1.4	2.2	1.2	2.2	2.8	3.4	3.7	3.7	3.8
	4G	3.0	2.7	1.8	0.5	1.8	1.8	0.8	1.0	0.7	0.6

Table 5. Average deviation between measurement and calculation power peaking factors by assembly types for Cycle 14 of Unit 4 ($\Delta=K_q^{meas}-K_q^{exp}$)·100

T_{ef}, [FPD]	Cycle, Assembly type	7.3	15	36	222.4	230	287.3	291
T_{in}, [°C]		263.5	263.5	263.1	260.6	263	263.9	260.8
H_{VI}, [cm]		197	178	198	185	201	205	160
N_t, [%]		100	100	100	50	100	100	55
Average Deviation, [%]	1G	-2.7	-2.4	-3.0	-7.9	-7.9	-9.1	-10.2
	2G	-9.2	-8.7	-9.1	-3.1	-4.3	-4.5	-3.4
	2D	-2.0	-2.2	-0.9	2.3	2.3	2.0	2.1
	3D	3.6	3.3	3.8	4.6	5.3	6.5	7.0
	4D	7.3	8.0	3.9	4.7	1.0	1.2	2.0

Table 6. Average deviation between measurement and calculation power peaking factors by assembly types for Cycle 15 of Unit 4 ($\Delta=K_q^{meas}-K_q^{exp}$)·100

T_{ef}, [FPD]	Cycle, Assembly type	1	13	39.8	86.7	135.2	174	198	240	306	330
T_{in}, [°C]		259.4	265.3	265.7	261.9	262.8	263.7	265.4	264.5	263.6	259.1
H_{VI}, [cm]		187	179	181	185	200	185	199	201	198	250
N_t, [%]		50	100	100	46	58	100	100	100	100	50
Average Deviation, [%]	1G	-3.7	-1.3	-1.8	-3.4	-5.6	-7.4	-8.5	-9.5	-10.9	-12.5
	2G	-3.5	-3.8	-4.6	-1.4	-1.9	-2.0	-0.4	0.6	0.0	0.7
	3G	-3.3	-1.7	0.3	1.0	1.8	4.2	6.1	4.5	7.4	9.2
	3D	4.4	4.9	4.7	4.9	6.0	6.1	6.6	7.0	7.3	7.8
	4D	6.8	1.9	3.3	0.6	2.7	5.9	2.4	3.2	4.3	4.9

Table 7. Average deviation between measurement and calculation power peaking factors by assembly types for Cycle 17 of Unit 4 ($\Delta=K_q^{meas}-K_q^{exp}$)·100

T_{ef}, [FPD]	Cycle, Assembly type	0.1	3.4	45	64	92.5	143.5	197	231	266.2	304.6
T_{in}, [°C]		262.6	265.3	264.9	265	262.4	264.8	264.7	264.8	264.7	263.3
H_{VI}, [cm]		185	193	175	182	198	197	199	199	194	250
N_t, [%]		55	95	100	100	52	100	100	100	100	-91
Average Deviation, [%]	1G	2.3	3.0	2.0	1.5	0.8	-0.8	-2.2	-2.8	-3.8	-4.3
	2G	-5.3	-6.0	-5.1	-4.9	-2.2	-3.5	-2.5	-2.4	-1.5	-1.2
	3G	-0.4	-0.7	-0.6	-0.2	-0.9	0.2	1.4	1.4	1.7	2.0
	4G	4.9	5.9	5.4	5.7	2.1	6.2	4.9	5.9	5.1	5.0

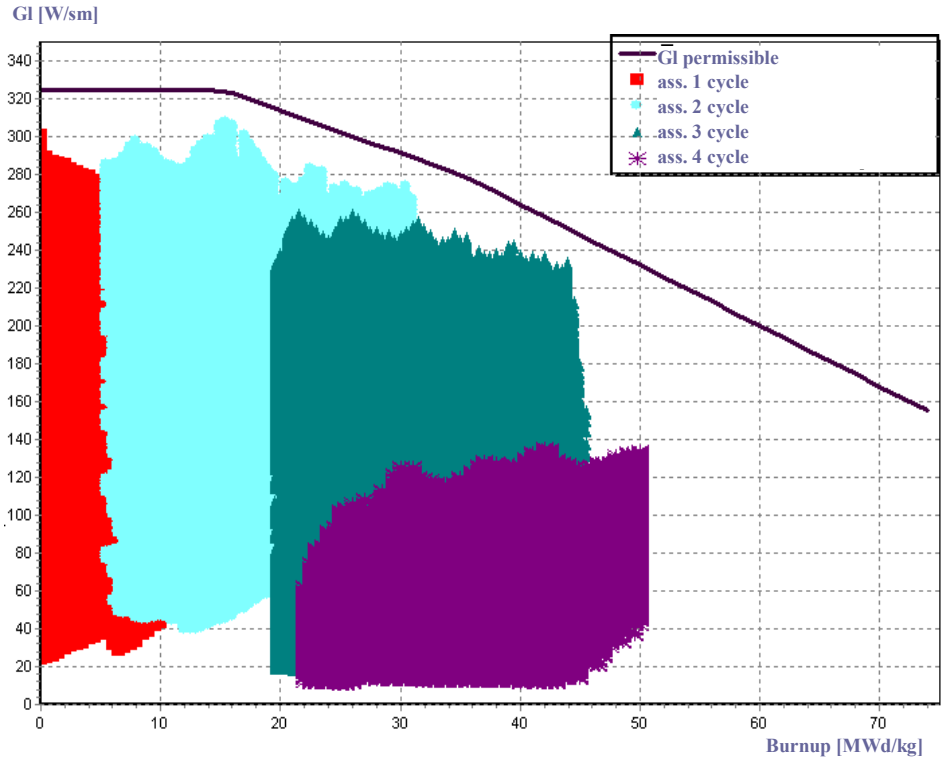

Figure 20. Permissible and calculation maximum linear power of WWER-440 – fuel rod for Cycle 16 of Unit 3

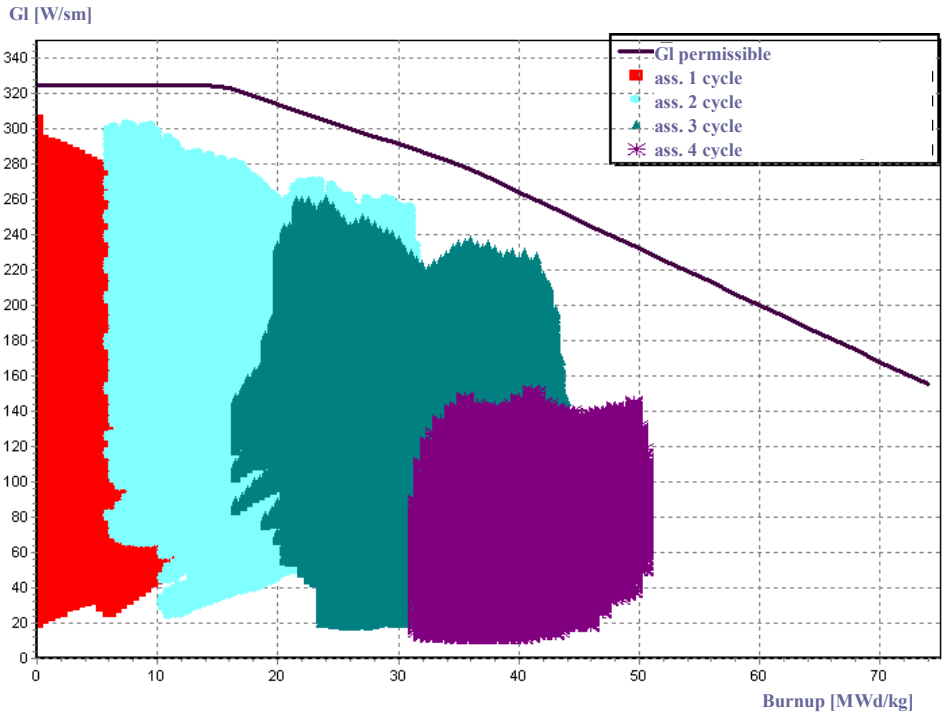

Figure 21. Permissible and calculation maximum linear power of WWER-440 – fuel rod for Cycle 17 of Unit 3

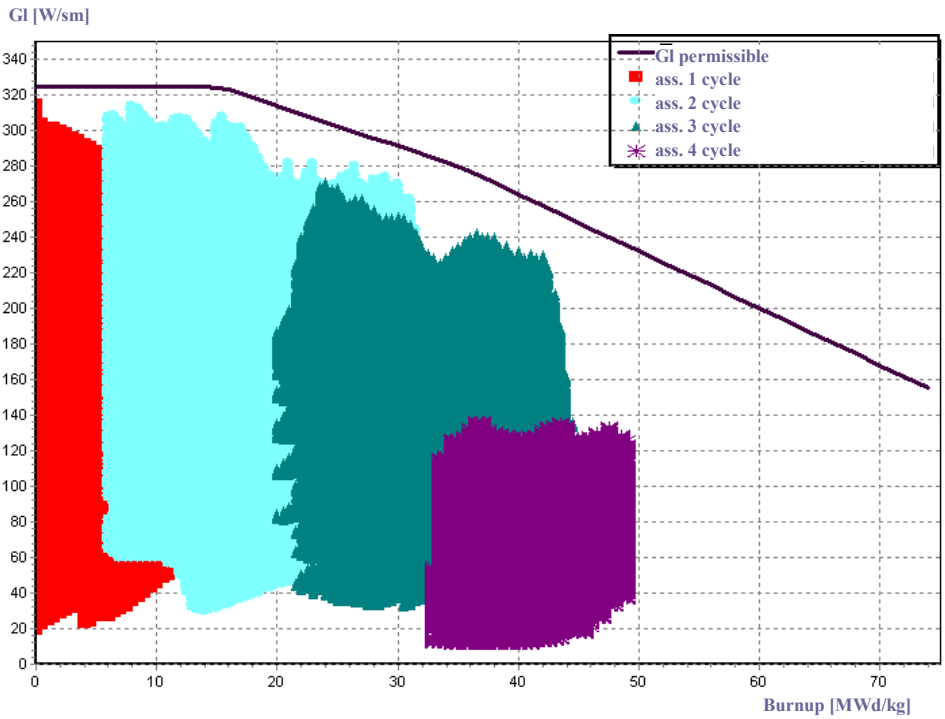

Figure 22. Permissible and calculation maximum linear power of WWER-440 – fuel rod for Cycle 18 of Unit 3

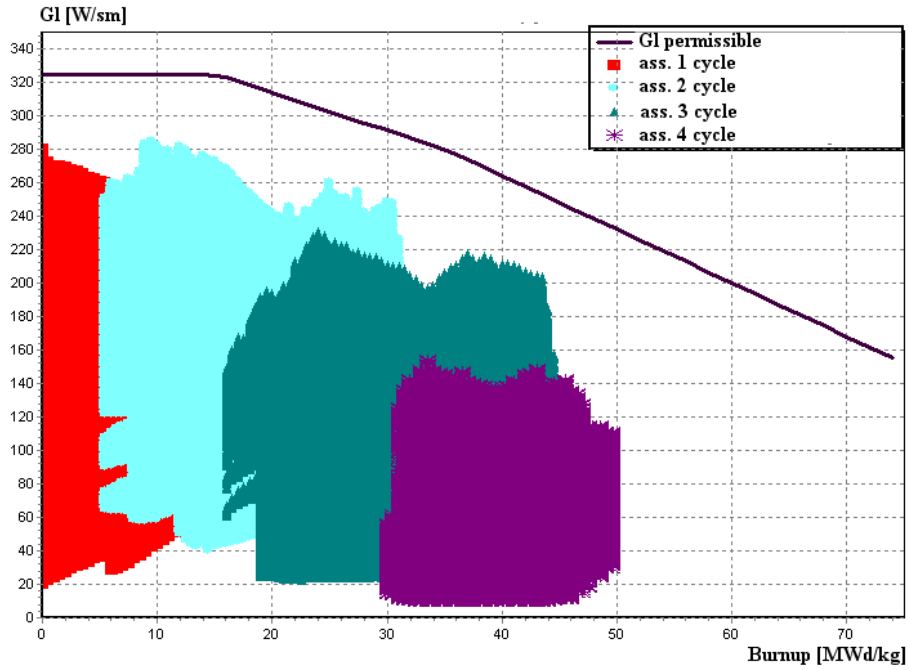

Figure 23. Permissible and calculation maximum linear power of WWER440 – fuel rod for Cycle 15 of Unit 4

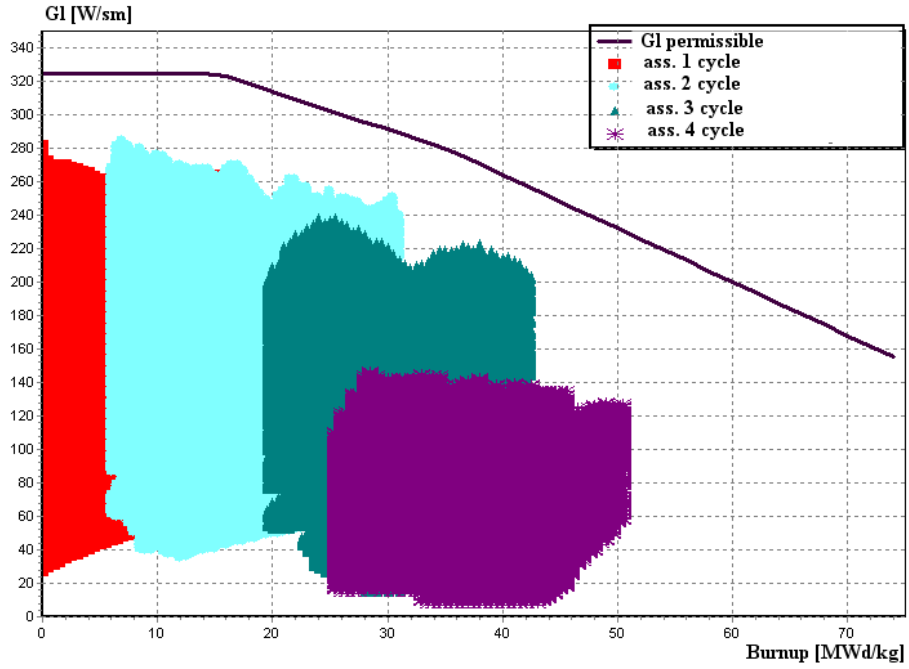

Figure 24. Permissible and calculation maximum linear power of WWER440 – fuel rod for Cycle 16 of Unit 4

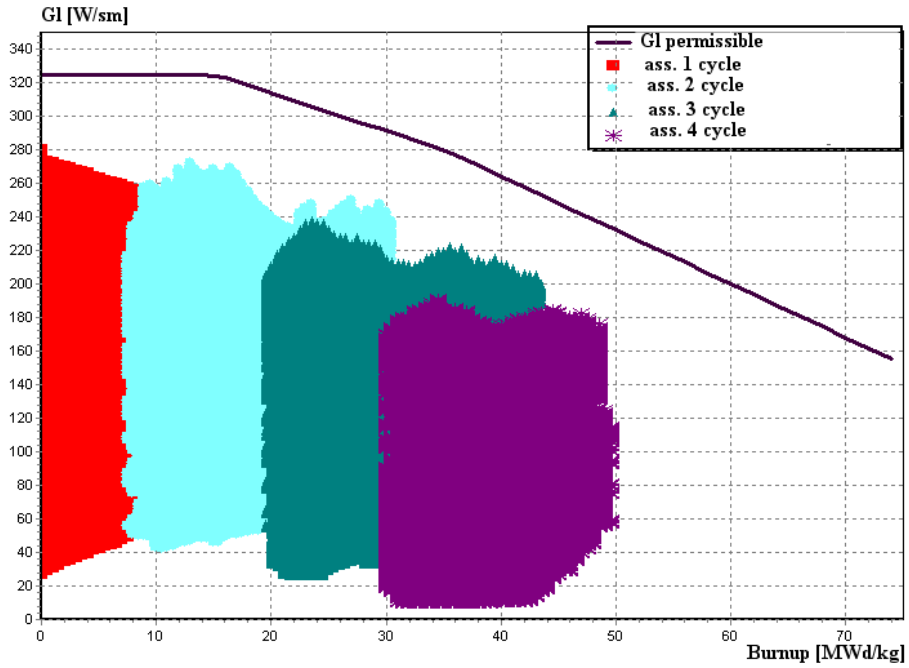

Figure 25. Permissible and calculation maximum linear power of WWER440 – fuel rod for Cycle 17 of Unit 4